

Exploration on flotation behavior of galena in seawater and related mechanism

Ningbo Song^{1,2,3}, Chuanyao Sun^{1,3}, Wanzhong Yin^{1,2}, Jin Yao^{1,2}, Bin Yang^{1,4}

¹ School of Resources and Civil Engineering, Northeastern University, Shenyang 110819, China

² State Key Laboratory of Mineral Processing, Beijing 102628, China

³ BGRIMM Technology Group, Beijing 100160, China

⁴ School of Chemical Engineering and Technology, China University of Mining and Technology, Xuzhou 221116, China

Corresponding author: yinwanzhong@mail.neu.edu.cn (Wanzhong Yin)

Abstract: The utilization of seawater in mineral flotation is the future development trend because of the shortage of fresh water resources. However, at present, the flotation behavior and mechanism of galena in seawater are not clear. Therefore, this paper comprehensively carried out the effect mechanism of seawater on the flotation of galena. Micro-flotation results illustrated that the recovery of galena was higher in deionized water than that in 5×10^{-2} mol/L $MgCl_2$ solution, 1×10^{-2} mol/L $CaCl_2$ solution and seawater. Contact angle determination and Zeta potential distribution measurements showed that hydrophilic substances adsorbed on the surface of galena under alkaline conditions. X-ray photoelectron spectroscopy (XPS) analysis further indicated that these substances were hydroxides precipitates, carbonate precipitates and hydroxyl complexes formed by divalent magnesium and calcium ions, which prevented the adsorption of collector on mineral surface. As a result, the galena recovery declined in 5×10^{-2} mol/L $MgCl_2$ solution, 1×10^{-2} mol/L $CaCl_2$ solution and seawater.

Keywords: high-sulfur magnetite, pyrrhotite flotation, magnetic separation, mixed collectors

1. Introduction

Mineral flotation consumes a large amount of fresh water resources. Due to the scarcity of fresh water resources, seawater is more and more widely used in mineral flotation (Byrne et al., 2012; Li et al., 2019b; Wang and Peng, 2014). At present, seawater flotation is mostly used in Chile and other coastal countries with relatively rich copper resources (Jeldres et al., 2016; Song et al., 2020).

The flotation behaviors of sulfide minerals in seawater are affected by many factors. The high concentration of electrolyte in seawater can reduce bubble size, enhanced foam stability (Castro et al., 2013; Chang et al., 2018). In addition, the high concentration of electrolyte compress the double electric layer on the surface of bubbles and mineral particles, thus reducing the slime cover on particles (Peng and Bradshaw, 2012; Zhang et al., 2015a; Zhang et al., 2015b) and promoting the adhesion of bubbles to mineral particles (Castro and Laskowski, 2011; Laskowski and Castro, 2015; Laskowski and Yoon, 1991). All the above can have a beneficial effect on sulfide minerals flotation. While on the other, seawater also has an adverse effect on sulfide minerals flotation. It's reported that the magnesium/calcium precipitation or hydroxyl complexes could adsorb onto the molybdenite (Ai et al., 2021; Castro et al., 2016; Chen et al., 2021; Lucay et al., 2015; Qiu et al., 2016; Ramirez et al., 2020a; Ramirez et al., 2020b; Rebolledo et al., 2017) and chalcopyrite (Li and Li, 2019; Li et al., 2019a; Li et al., 2017; Li et al., 2018; Mu and Peng, 2019a, b; Ramirez et al., 2018) surface at a high pH range to reduce the hydrophobicity of sulfide mineral surfaces. These phenomena are the main reasons for the decline of floatability of sulfide minerals in seawater.

Galena is the most important ingredient for industrial lead extraction, and it is a relatively common mineral, which is most suitable for flotation separation because of its good natural hydrophobicity. Galena flotation consumes a large amount of fresh water resources. Global identified lead resources amount to 1.5 billion tons, with 80 million tons of lead reserves, mainly distributed in Australia, China,

Russia, Peru, the United States and Mexico. Most of these countries are close to the ocean and have abundant and convenient seawater resources. Using seawater instead of fresh water to galena flotation will alleviate the shortage of fresh water resources largely. Up to now, however, the flotation behavior of galena in seawater and related mechanism has not been reported. The study of the effect of seawater on galena flotation can enrich the theoretical system of seawater replacing fresh water in sulfide mineral flotation, and contribute to a more comprehensive understanding of the related mechanism. Therefore, it is of great significance to carry out the study of galena flotation in seawater.

In order to clearly analyze the respective influence of divalent magnesium and calcium ions, this paper carried out the flotation of galena in 5×10^{-2} mol/L $MgCl_2$ solution, 1×10^{-2} mol/L $CaCl_2$ solution and seawater respectively, compared with the flotation of galena in deionized water. The concentration of $MgCl_2$ and $CaCl_2$ solutions were calculated according to the concentration of divalent magnesium and calcium ions in seawater. The galena flotation behavior and mechanism in four solutions were explored by micro-flotation experiments, contact angle determination, Zeta potential measurements and XPS analysis.

2. Materials and methods

2.1. Materials

The natural high purity galena sample used in this study was obtained from Guangxi Province, China. Galena samples with two different grain sizes were prepared, i.e. $-74+38 \mu m$ and $-38 \mu m$ particles. Samples with $-74+38 \mu m$ grain size were vacuumized and reserved for X-ray diffraction (XRD, X'Pert PRO MPD), XPS analysis and micro-flotation test. Additionally, $-38 \mu m$ samples were further ground to less than $5 \mu m$ and used for the zeta potential measurements. XRD and chemical composition analysis of the samples were carried out to evaluate the purity. The results are shown in Table 1 and Fig. 1, respectively. Synthetic seawater was prepared in laboratory on the basis of the research findings of Kester et al. (1967), and the main ions concentration was shown in Table 2.

Table 1. Chemical compositions of the pure galena samples (wt. %)

Components	Pb	S	Others
Contents	85.4	13.2	1.4

Table 2. The concentrations of main ions in the synthetic seawater (g/L)

Na^+	K^+	Ca^{2+}	Mg^{2+}	Cl^-	SO_4^{2-}	HCO_3^-
11.60	0.50	0.41	1.31	19.58	2.62	0.15

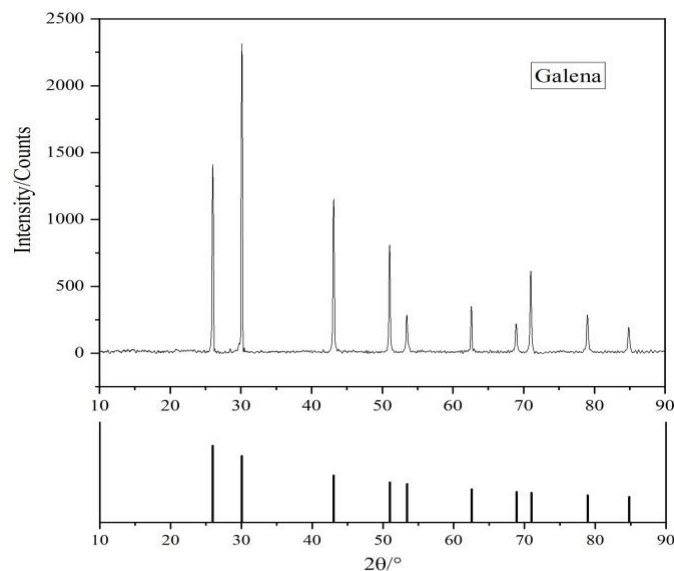


Fig.1. XRD pattern of pure galena samples

2.2. Micro-flotation experiments

A XFG flotation machine produced by Jilin Exploration Machinery Factory in China was used for micro-flotation at a spindle speed of 1992 rpm. 2.0 g galena and appropriate amount of deionized water were mixed and added to a 30ml flotation cell. In order to disperse galena evenly in the solution, the pulp in the flotation cell was stirred continuously for 1 minute. Deionized water with resistivity no less than $18.2\text{m}\Omega\cdot\text{cm}$ was produced by XJG-20-A Ultra-pure Water Device (Xinjie Technology Co., LTD., Shenyang, China) (Yang et al., 2021). The pH value of pulp was adjusted by HCl and NaOH. Sodium diethyl dithiocarbamate (DDTC) (purity, 98%) procured from Macklin Biochemical Co., LTD., (Shanghai, China) was used as collector. Methyl isobutyl carbinol (MIBC) (purity, 99%) procured from Aladdin Co., LTD., (Shanghai, China) was used as frother. The pulp was stirred for 2 min after the pH value was stabilized. DDTC (stirred for 3 minutes) and MIBC (stirred for 1 minute) were successively added, and then began manual scraping for 3 minutes. Concentrate and tailings were collected, dried and weighed respectively. The flotation recovery of galena can be directly calculated by the weight of concentrate and tailings. The experiment process is shown in Fig. 2.

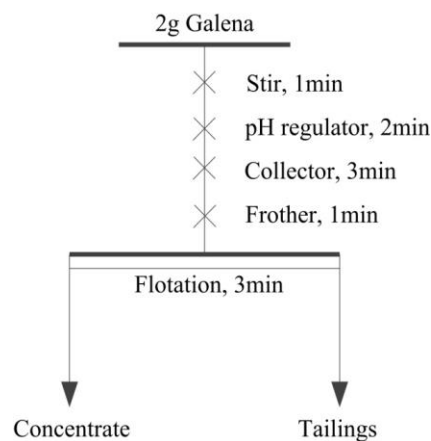


Fig.2. Flowchart of micro-flotation experiments

2.3. Contact angle determination

Contact angle determination is usually used to measure the surface wettability of minerals. Contact angles of galena before and after acting with collector in four solutions were measured in this test. Powder Tablet Method is the most frequently used sample preparation method when measuring the contact angle of powder sample (Sun et al., 2021; Zhu et al., 2020). In each measurement, 2.0 g galena sample was added into 40 mL solutions. Pure mineral samples were treated under the identical conditions as the micro-flotation experiments. After treatment, the samples were dried at 45°C for 36 h, and then pressed into wafers with a thickness of 1-2 mm with a pressure of 20 MPa, and the pressure was maintained for 1 min. The contact angle was detected using the Contact Angle Measuring Instrument (JC2000A, Powereach, Shanghai, China), and it was done by dropping water droplets with the diameter of about 2 to 3 mm on the sample surface with a micro syringe. Each experiment was performed more than three times, and the mean and standard deviation were recorded to determine the contact angle from the captured liquid-solid-gas contact interface profile (Sheng et al., 2021; Yang et al., 2020).

2.4. Zeta potential distribution measurements

Measurements of zeta potentials of galena in 5×10^{-2} mol/L MgCl_2 solution, 1×10^{-2} mol/L CaCl_2 solution, seawater and deionized water were carried out using an analyzer named Nano ZS90 which was made in Malvern Group, respectively. 20 mg samples were weighed and mixed to 30 mL electrolyte solution with a concentration of 1×10^{-3} mol/L KCl and stirred with a magnetic stirrer in each measurement. The order and interval time of reagent addition in the process of stirring were consistent with that in flotation experiment. After the stirring, the suspension stood for 10 min, and then the supernatant was

immited into the detection tank to measure the Zeta potential. Repeat the measurement three times for each sample to calculate the average as appropriate results.

2.5. XPS analysis

The preparation method of XPS sample in this paper was in accord with that employed in the micro-flotation experiments at pH 9.00. The prepared samples were filtered and rinsed for three times, then dried in a 45°C oven for test. A US-made Thermo KAlpha (ESCALAB 250 XI) X-ray photoelectron spectrometer was used to perform XPS detection. The Al K α microfocus monochromatic source size was 5 μ m and the data acquisition power was 72 W. The vacuum degree in the analysis room was less than or equal to 2×10^{-7} mbar. The pass energies of full-spectrum and narrow-spectrum scanning were 100eV and 50eV, and the energy scan step sizes were 1eV and 0.1eV, respectively. Standard C1s peak (284.8eV) was used to calibrate the acquired spectra and Thermo Vantage software was used to analyze the data.

3. Results and discussions

3.1. Micro-flotation results

Fig. 3 shows the galena recovery as a function of pH value in 5×10^{-2} mol/L MgCl₂ solution, 1×10^{-2} mol/L CaCl₂ solution, seawater and deionized water. The dosage of collector DDTc was 50 mg/L and frother MIBC was 40 mg/L. The results show that in deionized water, galena has good floatability at pH less than 9.00. Galena recovery decreased sharply when pH was higher than 9.00. Seawater had a positive effect on galena flotation under strong acid condition. When pH was higher than 4.7, the galena recovery in seawater was obviously lower than that in deionized water. When pH was 9.00, the recoveries of galena in 5×10^{-2} mol/L MgCl₂ solution, 1×10^{-2} mol/L CaCl₂ solution and seawater were 11.42%, 17.57% and 20.42%, respectively, which were much lower than 55.25% in deionized water.

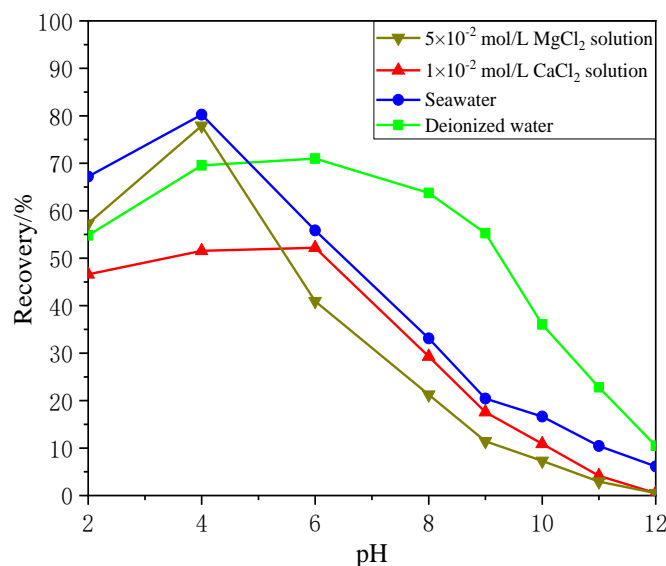


Fig. 3. Effect of pH value on galena recovery (CDDTC=50 mg/L, CMIBC=40 mg/L)

3.2. Contact angle measurements

The poor floatability of a mineral is due to decrease in surface hydrophobicity. Therefore, the contact angle test was carried out in order to reveal the mechanism of mineral flotation behavior. Fig. 4 shows the contact angle of galena with and without the action of collector in four different solutions, revealing the change of surface hydrophobicity of galena. The contact angles of galena in 5×10^{-2} mol/L MgCl₂ solution, 1×10^{-2} mol/L CaCl₂ solution, seawater and deionized water increased successively at pH 9.00, which were 62.9°, 65.7°, 72.1° and 81.4°, respectively. With the addition of collector, the contact angles of the four solutions were increased to 72.2°, 75.1°, 81.8° and 88.3°, respectively. The contact angle test

shows that the hydrophilic of galena decreases successively in 5×10^{-2} mol/L MgCl_2 solution, 1×10^{-2} mol/L CaCl_2 solution, seawater and deionized water.

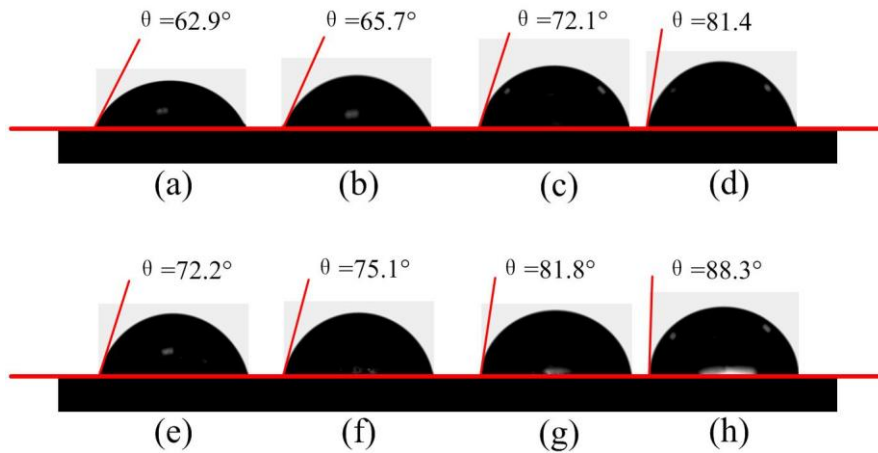


Fig. 4. Contact angles of galena before collector action in 5×10^{-2} mol/L MgCl_2 solution (a), 1×10^{-2} mol/L CaCl_2 solution (b), seawater (c) and deionized water (d). Contact angles of galena after collector action in 5×10^{-2} mol/L MgCl_2 solution (e), 1×10^{-2} mol/L CaCl_2 solution (f), seawater (g) and deionized water (h) (CDDTC=50 mg/L, CMIBC=40 mg/L)

3.3. Zeta potential distribution measurements

The adsorption of certain chemicals on mineral interfaces can change the electrical properties of mineral surfaces, as demonstrated by zeta potential measurement (Wang et al., 2022). Such substances can be molecules, ions, hydroxyl complexes, etc. Fig. 5 shows Zeta potentials of galena in four solutions at the pH range of 2.00~12.00. Compared with deionized water, the Zeta potential of galena in 5×10^{-2} mol/L MgCl_2 solution, 1×10^{-2} mol/L CaCl_2 solution and seawater moved in the positive direction when the pH was greater than 6.00, indicating that there was positively charged substance adsorption on the surface of galena. At pH 9.00, Zeta potentials of galena in 5×10^{-2} mol/L MgCl_2 solution, 1×10^{-2} mol/L CaCl_2 solution, seawater and deionized water were 8.24 mV, 0.31 mV, -0.53 mV and -12.43 mV, respectively. The positive movement of Zeta potential was most obvious in 5×10^{-2} mol/L MgCl_2 solution, indicating that positively charged substances adsorb most on galena surface. XPS analysis was carried out to confirm the species adsorbed on the galena surface in the following chapters.

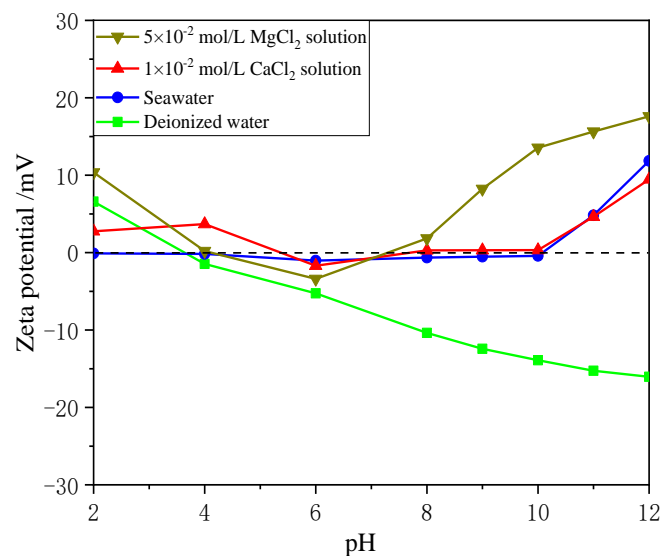


Fig.5. Effects on zeta potentials of galena as a function of pH value in 5×10^{-2} mol/L MgCl_2 solution, 1×10^{-2} mol/L CaCl_2 solution, seawater and deionized water

3.4. XPS analysis

According to Fig. 6 and Table 3, the atomic concentration of lead on the surface of galena in deionized water is higher than that in 5×10^{-2} mol/L MgCl_2 solution, 1×10^{-2} mol/L CaCl_2 solution and seawater. The atomic concentration of magnesium on the surface of galena was 3.24% in 5×10^{-2} mol/L MgCl_2 solution and 1.97% in seawater. Meanwhile, the atomic concentration of calcium on the surface of galena was 0.83% in 1×10^{-2} mol/L CaCl_2 solution and 0.75% in seawater. The changes of the atomic concentrations confirmed the adsorption of precipitates and hydroxyl complexes containing magnesium or calcium covering galena surfaces in 5×10^{-2} mol/L MgCl_2 solution, 1×10^{-2} mol/L CaCl_2 solution and seawater.

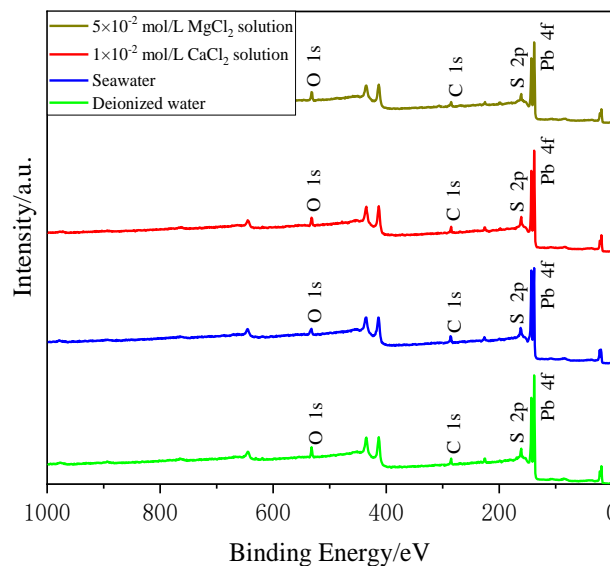


Fig. 6. The XPS spectra of galena in 5×10^{-2} mol/L MgCl_2 solution, 1×10^{-2} mol/L CaCl_2 solution, seawater and deionized water

Table 3. Atomic concentration of main elements on the surface of galena

Samples	Atomic concentration/%					
	Pb 4f	S 2p	C 1s	O 1s	Ca 2p	Mg 1s
5×10^{-2} mol/L MgCl_2 .	19.23	16.11	35.92	25.50	--	3.24
1×10^{-2} mol/L CaCl_2	20.27	18.48	38.56	21.86	0.83	--
Seawater	18.24	16.90	43.44	18.70	0.75	1.97
Deionized water	22.97	19.28	33.21	21.90	--	--

As shown in Fig. 7, Mg 1s peak appeared at around 1302.75 eV in 5×10^{-2} mol/L MgCl_2 solution and at around 1302.73 eV in seawater, respectively. These results confirmed that there were $\text{Mg}(\text{OH})_{2(s)}$ precipitation and $\text{Mg}(\text{OH})^+$ complexes (Haycock et al., 1978) adsorption on galena surface in 5×10^{-2} mol/L MgCl_2 solution and seawater.

As shown in Fig. 8, Ca 2p_{3/2} peak appeared in 1×10^{-2} mol/L CaCl_2 solution and seawater at 347.58 eV and 346.96 eV, and Ca 2p_{1/2} peak appeared in 1×10^{-2} mol/L CaCl_2 solution and seawater at 350.70 eV and 350.64 eV, respectively. These results confirmed that there were $\text{CaCO}_{3(s)}$ precipitation (Christie et al., 1983) and $\text{Ca}(\text{OH})^+$ complexes (Sugama et al., 1989) adsorption on galena surface in 1×10^{-2} mol/L CaCl_2 solution and seawater.

In order to further investigate the adverse effects of hydrophilic substances on the adsorption of collector on galena surface in four solutions, XPS analysis was carried out on galena treated with DDTC. In XPS spectrum, the atomic concentration has a linear relationship with the corresponding peak area, so the element content can be expressed qualitatively by the area of the spectral peak.

In XPS spectrum, there is a linear relationship between the spectral peak area and the atomic concentration in the sample. Therefore, the area of an atomic spectral peak can be used as a rough repre-

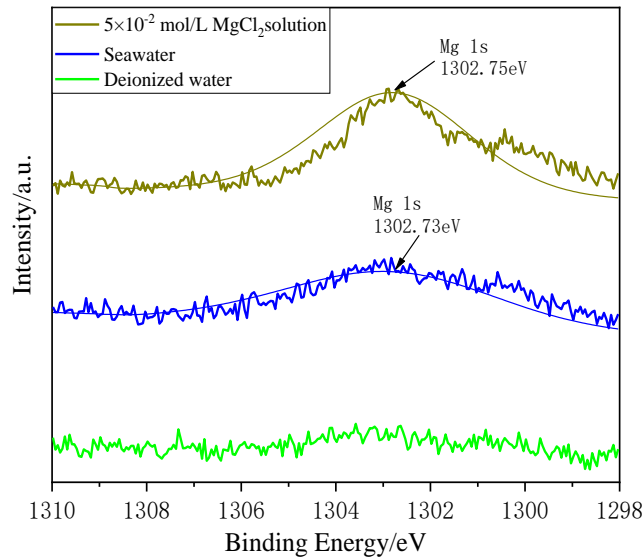


Fig. 7. Mg 1s X-ray photoelectron spectra of galena surface in 5×10^{-2} mol/L MgCl_2 solution, seawater and deionized water

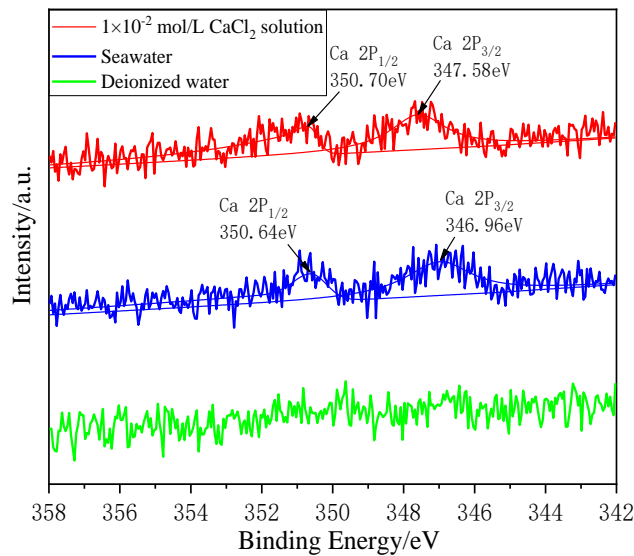


Fig. 8. Ca 2p X-ray photoelectron spectra of galena surface in 1×10^{-2} mol/L CaCl_2 solution, seawater and deionized water

sentation of concentration (Zhang et al., 2022). As shown in Fig. 9 and Table 4, N peak areas in 5×10^{-2} mol/L MgCl_2 solution, 1×10^{-2} mol/L CaCl_2 solution, seawater and deionized water are 3073.84, 2780.43, 3135.52 and 3273.23 and the atomic content of N are 2.78%, 2.75%, 3.43% and 3.60%, respectively. It can be considered that compared with deionized water, the adsorption of DDTC (Achilleos et al., 1989) on galena surface decreases in 5×10^{-2} mol/L MgCl_2 solution, 1×10^{-2} mol/L CaCl_2 solution and seawater.

Table 4. Content of N in different solutions on the surface of galena treated with DDTC

Samples	N area / eV	Atomic / %
5×10^{-2} mol/L MgCl_2	3073.84	2.78
1×10^{-2} mol/L CaCl_2	2780.43	2.75
Seawater	3135.52	3.43
Deionized water	3273.23	3.60

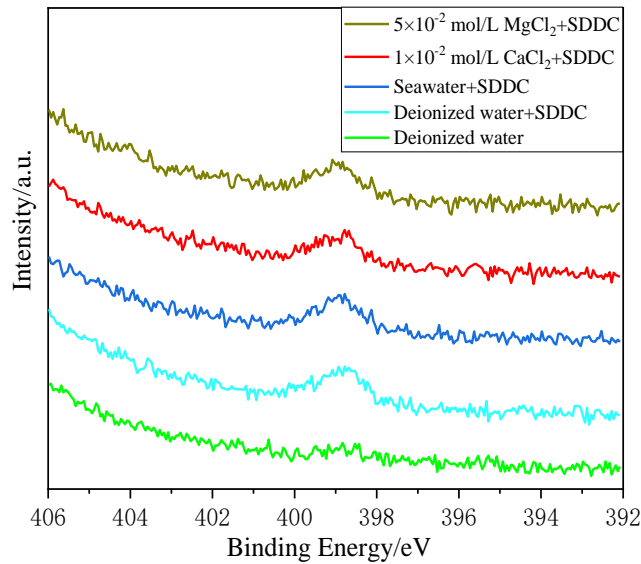


Fig. 9. N 1s X-ray photoelectron spectra of galena treated with DDTC in 5×10^{-2} mol/L MgCl_2 solution, 1×10^{-2} mol/L CaCl_2 solution, seawater and deionized water

3.5. Discussion

DDTC is an anionic-heteropolar-sulphydryl collector. The hydrophilic groups produced by the dissociation of the collector in water interact with the mineral surface so that the collector adsorbs on the mineral surface. As shown in Fig. 10 (d), Lead atoms on galena surface reacts with $(\text{C}_2\text{H}_5)_2\text{NCSS}^-$ to form lead diethyldithiocarbamate. Therefore, the adsorption method of DDTC on galena is chemical adsorption (Su, 2012). Under alkaline conditions, As shown in Fig. 10 (a, b, c), $\text{Mg}(\text{OH})_{2(\text{s})}$ precipitation and $\text{Mg}(\text{OH})^+$ complexes were formed in 5×10^{-2} mol/L MgCl_2 solution, $\text{CaCO}_{3(\text{s})}$ precipitation and $\text{Ca}(\text{OH})^+$ complexes were formed in 1×10^{-2} mol/L CaCl_2 solution, and $\text{Mg}(\text{OH})_{2(\text{s})}$, $\text{CaCO}_{3(\text{s})}$ precipitation and $\text{Mg}(\text{OH})^+$, $\text{Ca}(\text{OH})^+$ complexes were formed in seawater. According to the speciation calculation by Peng (Peng et al., 2020) et al., no $\text{Ca}(\text{OH})_{2(\text{s})}$ precipitate was generated in experiments due to the pH value lower than 12. The hydrophilic substances cover and then inhibit the adsorption of DDTC on the surface of galena, thus reducing the galena recovery.

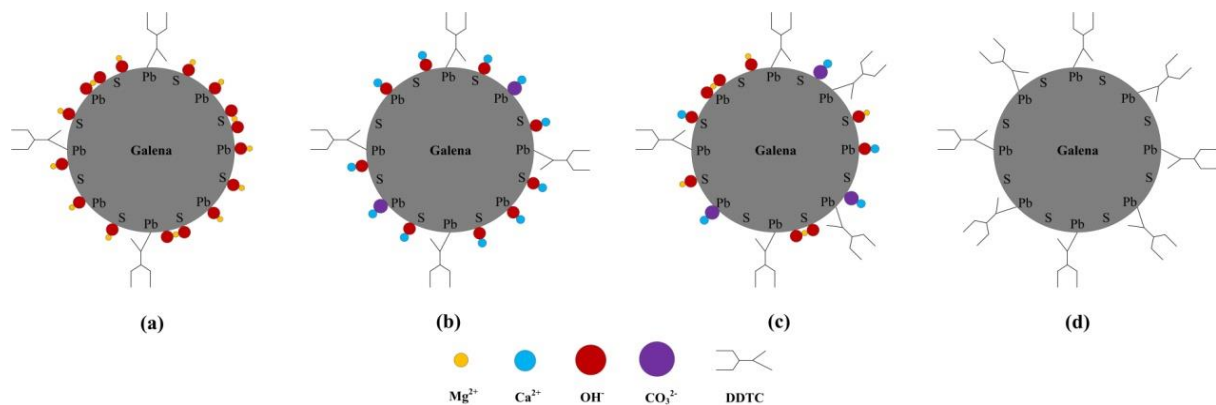


Fig. 10. Schematic diagram of adsorption models of DDTC on galena in 5×10^{-2} mol/L MgCl_2 solution (a), 1×10^{-2} mol/L CaCl_2 solution (b), seawater(c) and deionized water (d)

4. Conclusions

This study investigates the effect mechanism of seawater on galena flotation by micro-flotation experiments, contact angle determination, Zeta potential distribution measurements and XPS analysis. The result of micro-flotation experiment shows that when pH is higher than 9.00, the flotation recoveries of galena in 5×10^{-2} mol/L MgCl_2 solution, 1×10^{-2} mol/L CaCl_2 solution and seawater decrease sharply,

which are much lower than that in deionized water. Contact angles measurements demonstrate that the hydrophobicity of galena increased successively in 5×10^{-2} mol/L MgCl_2 solution, 1×10^{-2} mol/L CaCl_2 solution, seawater and deionized water. Zeta potential distribution measurements confirm that positively charged substances adsorb on the galena surface in 5×10^{-2} mol/L MgCl_2 solution, 1×10^{-2} mol/L CaCl_2 solution and seawater. XPS analysis tests further illustrate that the adsorbed substances are $\text{Mg}(\text{OH})_{2(s)}$ precipitation and $\text{Mg}(\text{OH})^+$ complexes in 5×10^{-2} mol/L MgCl_2 solution, $\text{CaCO}_{3(s)}$ precipitation, $\text{Ca}(\text{OH})^+$ complexes in 1×10^{-2} mol/L CaCl_2 solution, and $\text{Mg}(\text{OH})_{2(s)}$, $\text{CaCO}_{3(s)}$ precipitation and $\text{Mg}(\text{OH})^+$, $\text{Ca}(\text{OH})^+$ complexes in seawater.

In general, seawater has an adverse effect on galena flotation due to the presence of divalent magnesium and calcium ions and the effect of divalent magnesium ions is greater than that of divalent calcium ions. It can be considered that the floatability of galena is reduced due to adsorption of hydrophilic hydroxide precipitates, carbonate precipitates and hydroxyl complexes on the surface under alkaline conditions.

Acknowledgments

The authors are grateful for the financial support by the Open Foundation of State Key Laboratory of Mineral Processing (GRANT No. BGRIMM-KJSKL-2021-23), the National Natural Science Foundation of China (GRANT No. 52174239, 51974064), and the Fundamental Research Funds for the Central Universities, China (GRANT No. N2101025).

References

- ACHILLEOS, A.A., GAHAN, L.R., HAMBLEY, T.W., HEALY, P.C., WEEDON, D.M., 1989. *Structural and x-ray photoelectron spectroscopic properties of hydrophobic cobalt(III) 'Cage' complexes with dithiocarbamate anions*. *Inorganica Chimica Acta*. 157, 209-214.
- AI, G., HUANG, K., LIU, C., YANG, S., 2021. *Exploration of amino trimethylene phosphonic acid to eliminate the adverse effect of seawater in molybdenite flotation*. *International Journal of Mining Science and Technology*. 31, 1129-1134.
- BYRNE, P., WOOD, P.J., REID, I., 2012. *The Impairment of River Systems by Metal Mine Contamination: A Review Including Remediation Options*. *Crit. Rev. Environ. Sci. Technol.*. 42, 2017-2077.
- CASTRO, S., LASKOWSKI, J.S., 2011. *Froth Flotation in Saline Water*. *Powder & Particle*. 29, 4-15.
- CASTRO, S., LOPEZ-VALDIVIESO, A., LASKOWSKI, J.S., 2016. *Review of the flotation of molybdenite. Part I: Surface properties and floatability*. *International Journal of Mineral Processing*. 148, 48-58.
- CASTRO, S., MIRANDA, C., TOLEDO, P., LASKOWSKI, J.S., 2013. *Effect of frothers on bubble coalescence and foaming in electrolyte solutions and seawater*. *International Journal of Mineral Processing*. 124, 8-14.
- CHANG, Z.Y., CHEN, X.M., PENG, Y.J., 2018. *The effect of saline water on the critical degree of coal surface oxidation for coal flotation*. *Minerals Engineering*. 119, 222-227.
- CHEN, Y., CHEN, X., PENG, Y., 2021. *The depression of molybdenite flotation by sodium metabisulphite in fresh water and seawater*. *Minerals Engineering*. 168, 106939.
- CHRISTIE, A.B., LEE, J., SUTHERLAND, I., WALLS, J.M., 1983. *An XPS study of ion-induced compositional changes with group II and group IV compounds*. *Applications of Surface Science*. 15, 224-237.
- HAYCOCK, D.E., KASRAI, M., NICHOLLS, C.J., URCH, D.S., 1978. *The electronic structure of magnesium hydroxide (brucite) using X-ray emission, X-ray photoelectron, and auger spectroscopy*. *Journal of the Chemical Society, Dalton Transactions*. 1791-1796.
- JELDRES, R.I., FORBES, L., CISTERMAS, L.A., 2016. *Effect of Seawater on Sulfide Ore Flotation: A Review*. *Mineral Processing and Extractive Metallurgy Review*. 37, 369-384.
- KESTER, D.R., DUEDALL, I.W., CONNORS, D.N., PYTKOWICZ, R.M., 1967. *Preparation of artificial seawater*. 12, 176-179.
- LASKOWSKI, J., CASTRO, S., 2015. *Flotation in concentrated electrolyte solutions*. *International Journal of Mineral Processing*. 144, 50-55.
- LASKOWSKI, J.S., YOON, R.-H., 1991. *Energy Barrier in Particle to Bubble Attachment and its Effect on Flotation Kinetics*. XVII International Minerals Processing Congress. 237-249.
- LI, W., LI, Y., 2019. *Improved understanding of chalcopyrite flotation in seawater using sodium hexametaphosphate*. *Minerals Engineering*. 134, 269-274.

- LI, Y., ZHU, H., LI, W., ZHU, Y., 2019a. *A fundamental study of chalcopyrite flotation in sea water using sodium silicate*. Minerals Engineering. 139, 105862.
- LI, Y.B., XIE, S.B., ZHAO, Y.L., XIA, L., LI, H.Q., SONG, S.X., 2019b. *The Life Cycle of Water Used in Flotation: a Review*. Mining Metall. Explor.. 36, 385-397.
- LI, Y.B., LI, W.Q., XIAO, Q., HE, N., REN, Z.J., Lartey, C., Gerson, A.R., 2017. *The Influence of Common Monovalent and Divalent Chlorides on Chalcopyrite Flotation*. Minerals. 7.
- LI, Z., RAO, F., SONG, S., LI, Y., LIU, W., 2018. *Slime coating of kaolinite on chalcopyrite in saline water flotation*. International Journal of Minerals, Metallurgy, and Materials. 25, 481-488.
- LUCAY, F., CISTERNAS, L.A., GALVEZ, E.D., A., L.-V., 2015. *Study of the natural floatability of molybdenite fines in saline solutions and effect of gypsum precipitation*. Minerals & Metallurgical Processing. 32, 203-208.
- MU, Y., PENG, Y., 2019a. *The effect of saline water on copper activation of pyrite in chalcopyrite flotation*. Minerals Engineering. 131, 336-341.
- MU, Y., PENG, Y., 2019b. *The role of sodium metabisulphite in depressing pyrite in chalcopyrite flotation using saline water*. Minerals Engineering. 142, 105921
- PENG, Y., BRADSHAW, D., 2012. *Mechanisms for the improved flotation of ultrafine pentlandite and its separation from lizardite in saline water*. Minerals Engineering. 36-38, 284-290.
- PENG, Y., LI, Y.B., LI, W.Q., Fang, X., Liu, C., Fan, R., 2020. *Elimination of adverse effects of seawater on molybdenite flotation using sodium silicate*. Minerals Engineering. 146, 106108.
- QIU, Z., LIU, G., LIU, Q., Zhong, H., 2016. *Understanding the roles of high salinity in inhibiting the molybdenite flotation*. Colloids and Surfaces A: Physicochemical and Engineering Aspects. 509, 123-129.
- RAMIREZ, A., GUTIERREZ, L., LASKOWSKI, J.S., 2020a. *Use of "oily bubbles" and dispersants in flotation of molybdenite in fresh and seawater*. Minerals Engineering. 148, 106197.
- RAMIREZ, A., GUTIERREZ, L., VEGA-GARCIA, D., REYES-BOZO, L., 2020b. *The Depressing Effect of Kaolinite on Molybdenite Flotation in Seawater*. Minerals. 10, 578.
- RAMIREZ, A., ROJAS, A., GUTIERREZ, L., LASKOWSKI, J.S., 2018. *Sodium hexametaphosphate and sodium silicate as dispersants to reduce the negative effect of kaolinite on the flotation of chalcopyrite in seawater*. Minerals Engineering. 125, 10-14.
- REBOLLEDO, E., LASKOWSKI, J.S., GUTIERREZ, L., Castro, S., 2017. *Use of dispersants in flotation of molybdenite in seawater*. Minerals Engineering. 100, 71-74.
- SHENG, Q., YIN, W., YANG, B., CAO, S., SUN, H., MA, Y., CHEN, K., 2021. *Improving surface sulfidization of azurite with ammonium bisulfate and its contribution to sulfidization flotation*. Minerals Engineering. 171, 107072.
- SONG, N., SUN, C., YIN, W., YAO, J., YANG, B., LIU, X., 2020. *Genetic Characteristics Analysis of the Effect of Seawater on Mineral Flotation*. Metal Mine. 6, 2-8.
- SU, J., 2012. *Study of adsorption behavior and mechanism of heteropolar sulfhydryl collectors on galena*. Central South University.
- SUGAMA, T., KUKACKA, L.E., CARCIELLO, N., Hocker, N.J., 1989. *Study of interactions at water-soluble polymer/Ca(OH)₂ or gibbsite interfaces by XPS*. Cement and Concrete Research. 19, 857-867.
- SUN, H., YANG, B., ZHU, Z., YIN, W., SHENG, Q., HOU, Y., YAO, J., 2021. *New insights into selective-depression mechanism of novel depressant EDTMPS on magnesite and quartz surfaces: Adsorption mechanism, DFT calculations, and adsorption model*. Minerals Engineering. 160, 106660.
- WANG, B., PENG, Y.J., 2014. *The effect of saline water on mineral flotation - A critical review*. Minerals Engineering. 66-68, 13-24.
- WANG, X., ZHAO, B., LIU, J., ZHU, Y., HAN, Y., 2022. *Dithiouracil, a highly efficient depressant for the selective separation of molybdenite from chalcopyrite by flotation: Applications and mechanism*. Minerals Engineering. 175, 107287.
- YANG, B., YIN, W., ZHU, Z., SUN, H., SHENG, Q., FU, Y., YAO, J., ZHAO, K., 2021. *Differential adsorption of hydrolytic polymaleic anhydride as an eco-friendly depressant for the selective flotation of apatite from dolomite*. Separation and Purification Technology. 256, 117803.
- YANG, B., ZHU, Z., SUN, H., YIN, W., HONG, J., CAO, S., TANG, Y., ZHAO, C., YAO, J., 2020. *Improving flotation separation of apatite from dolomite using PAMS as a novel eco-friendly depressant*. Minerals Engineering. 156, 106492.
- ZHANG, J., ZHANG, X.-G., WEI, X.-X., CHENG, S.-Y., HU, X.-Q., LUO, Y.-C., XU, P.-F., 2022. *Selective depression of galena by sodium polyaspartate in chalcopyrite flotation*. Minerals Engineering. 180, 107464.

- ZHANG, M., PENG, Y.J., XU, N., 2015a. *The effect of sea water on copper and gold flotation in the presence of bentonite.* Minerals Engineering. 77, 93-98.
- ZHANG, M., XU, N., PENG, Y.J., 2015b. *The entrainment of kaolinite particles in copper and gold flotation using fresh water and sea water.* Powder Technology. 286, 431-437.
- ZHU, Z., YIN, W., WANG, D., SUN, H., CHEN, K., YANG, B., 2020. *The role of surface roughness in the wettability and floatability of quartz particles.* Applied Surface Science. 527, 146799.